



Cite this: *RSC Adv.*, 2023, **13**, 937

## Recent advances in $\text{g-C}_3\text{N}_4$ -based photo-enzyme catalysts for degrading organic pollutants

Yaohua Gu,<sup>1,†,a</sup> Siao Li,<sup>†,a</sup> Mingming Li,<sup>†,b</sup> Xinyu Wang,<sup>a</sup> Ying Liu,<sup>a</sup> Keren Shi,<sup>c</sup> Xiaoyan Bai,<sup>a</sup> Qing Yao,<sup>\*,a</sup> Zhiqiang Wu<sup>\*,d</sup> and Huiqin Yao<sup>1,\*,a</sup>

In recent years, photocatalytic reactions have shown great potential in degrading organic pollutants because of their simple operation and no secondary pollution. Graphitic carbon nitride ( $\text{g-C}_3\text{N}_4$ ) is one of the most frequently used photocatalyst materials in the field of photocatalysis because it is a form of photocatalytic material with facile synthesis, no metal, visible light response, and strong stability. Enzyme-catalyzed degradation has received extensive attention due to its broad selectivity, high efficiency, and environmental friendliness. Horseradish peroxidase (HRP), one of several oxidoreductases utilized for pollutant degradation, has a wide range of applications due to its mild reaction conditions and high stability. Exploring efficient platforms for immobilizing  $\text{g-C}_3\text{N}_4$  and HRP to develop photo-enzyme-coupled catalysis is an attractive practical topic. The coupling effect of  $\text{g-C}_3\text{N}_4$  and HRP improves the carrier separation efficiency and generates more active species, which finally realize the solar-driven non-selective destruction of organic pollutants. We describe the alteration of  $\text{g-C}_3\text{N}_4$  and the immobilization of HRP in detail in this study, and we outline recent developments in the photo-enzyme coupling of  $\text{g-C}_3\text{N}_4$  and HRP.

Received 4th November 2022  
Accepted 21st December 2022

DOI: 10.1039/d2ra06994f

[rsc.li/rsc-advances](http://rsc.li/rsc-advances)

### 1. Introduction

With the continuous progress of industrial and social development, the problem of water pollution has become increasingly prominent.<sup>1</sup> Coking wastewater, dye wastewater, pharmaceutical wastewater, pesticide wastewater and other industrial wastewater contain a large number of organic pollutants. Organic contaminants are not easily degraded by metabolic processes and perform poorly in biodegradation.<sup>2,3</sup> In addition, several of these chemicals are carcinogenic, teratogenic, and mutagenic, which may be hazardous to the environment and human health.<sup>4</sup> Given that, comprehensive and

<sup>a</sup>Key Laboratory of Environmental Factors and Chronic Disease Control, College of Public Health and Management, School of Basic Medicine, Ningxia Medical University, Yinchuan 750004, P. R. China. E-mail: [yaohq@nxu.edu.cn](mailto:yaohq@nxu.edu.cn); [yaoqing726@163.com](mailto:yaoqing726@163.com)

<sup>b</sup>Urology Surgery, General Hospital of Ningxia Medical University, Yinchuan 750004, P. R. China

<sup>c</sup>State Key Laboratory of High-efficiency Coal Utilization and Green Chemical Engineering, Ningxia University, Yinchuan 750021, P. R. China

<sup>d</sup>College of Chemistry and Chemical Engineering, Ningxia Normal University, Guyuan 756000, P. R. China. E-mail: [wuzqs@nxnu.edu.cn](mailto:wuzqs@nxnu.edu.cn)

† Contributed equally as first author.



Yaohua Gu received his BS (2013) and PhD (2019) degrees from Ningxia University, China. He is an associate professor at the key laboratory of environmental factors and chronic disease control of Ningxia Medical University. His current research interests include the development of photo-enzyme catalysts for degrading organic pollutants.



Siao Li received her BS degree in 2021 from Hebei University, China. She is currently studying for a MS degree at Ningxia Medical University. Her research interests focus on the study of biocatalytic degradation of pollutants.



novel research on organic pollutant degradation technology is critical to resolving such wastewater pollution issues.

Photocatalytic oxidation, ozone oxidation, and Fenton oxidation have all become research hotspots in treating residual chemicals because they can completely degrade organic contaminants into inorganic compounds like  $\text{CO}_2$  and  $\text{H}_2\text{O}$ . It is especially noticeable in the photocatalytic oxidation approach due to its simplicity, lack of secondary pollution generation, and excellent development potential. Photo catalysts can effectively mineralize organic pollutants into small molecules, such as  $\text{H}_2\text{O}$ ,  $\text{CO}_2$ ,  $\text{N}_2$ , etc. under photoreaction conditions,<sup>5</sup> and fundamentally eliminate secondary pollution.<sup>6</sup> Pham *et al.* prepared a cobalt-doped graphitic carbon nitride (Co/GCN) to enhance the photo-degradation of paracetamol (PC).<sup>7</sup> Through LC-MS analysis of the identification of intermediates, the reactive species including  $\cdot\text{O}_2^-$ ,  $\cdot\text{OH}$  and  $\text{h}^+$  can react with PC and decompose it into intermediates which are further oxidized to  $\text{CO}_2$  and  $\text{H}_2\text{O}$ . As a result, photocatalytic technology has become one of the most effective means to solve the current environmental deterioration.<sup>8</sup> Among many photo catalyst materials, graphitic carbon nitride ( $\text{g-C}_3\text{N}_4$ ) is one of the most promising photocatalytic materials, which is easy to be synthesized, contain no metals, has a good visible light response and good stability. Peroxidase enzymes promote the degradation of toxic environmental pollutants by reducing activation energy. Huang *et al.* introduced 2,2'-azide bis (3-ethylbenzothiazoline-6-sulfonate) (ABTS) into the Horseradish peroxidase/ $\text{H}_2\text{O}_2$  system to enhance the degradation of diclofenac at neutral pH.<sup>9</sup> Horseradish peroxidase (HRP) has many advantages in the biodegradation process: highly specific, rapid process, more flexible operating conditions, efficient degradation even under harmful environmental conditions, no nutrient supply and reduced by-product formation.<sup>10</sup> Due to the excellent water solubility, poor stability, and environmental sensitivity, free enzymes are difficult to reuse in practical applications.<sup>11</sup> The most effective method for enzyme reuse is immobilization to maximize the utilization of the enzyme.<sup>12</sup> Petronijevic *et al.* covalently immobilized HRP on Biochar (BC) supports phenol degradation. After 4 washes, the immobilized HRP retained more than 79% activity.<sup>13</sup>

The research results published so far show that the rational combination of photo catalysts and enzymes can be used to construct photo-enzyme-coupled catalytic systems, which can effectively improve the stability and reusability of the enzyme, increase the rate of photocatalytic reactions, and achieve complete degradation of pollutants.<sup>14,15</sup> In this review, we systematically analysed this complex catalytic system, clearly showing the photo enzyme coupled catalytic system. We summarize the modification of carbon nitride in photo catalysts and the immobilization of HRP in peroxidase. Then combined with the advantages of photo catalysis and enzyme catalysis, the photo-enzyme-coupled catalytic system formed by carbon nitride and HRP was systematically introduced.

## 2. Modification of $\text{g-C}_3\text{N}_4$

Fujishima *et al.* first proposed in 1972 that N-type semiconductor  $\text{TiO}_2$  could realize photocatalytic water splitting,<sup>16</sup> and Carey *et al.* reported in 1976 that  $\text{TiO}_2$  could realize photocatalytic oxidative dechlorination of PCBs.<sup>17</sup> Photocatalytic technologies have since been used to tackle environmental pollution successfully. Fig. 1 depicts the working principle of semiconductor photo catalyst degradation. In 2009, Wang *et al.* first reported that graphite phase carbon nitride ( $\text{g-C}_3\text{N}_4$ ) can be used as a stable photocatalyst to decompose water to produce hydrogen.<sup>18</sup> Since then,  $\text{g-C}_3\text{N}_4$  has received more and more attention from scholars at home and abroad. Fig. 2 shows the

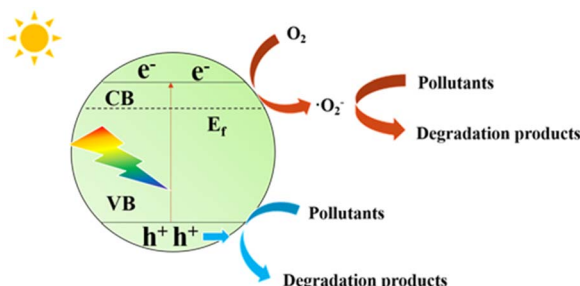


Fig. 1 The working principle of photocatalyst degradation.



*Qing Yao received her BS degree in 1998 from Ningxia Medical University and PhD degree in 2012 from Beijing University of Traditional Chinese Medicine, China. She is a professor of Biochemistry at Ningxia Medical University. Her current research interests include the development of enzyme catalysis for degrading organic pollutants.*



*Huiqin Yao received her BS degree in 2002 from Ningxia University and PhD degree in 2011 from Beijing Normal University, China. She is a professor of Medical Chemistry at Ningxia Medical University. Her current research interests include the development of enzyme catalysis for nanomaterials applications.*



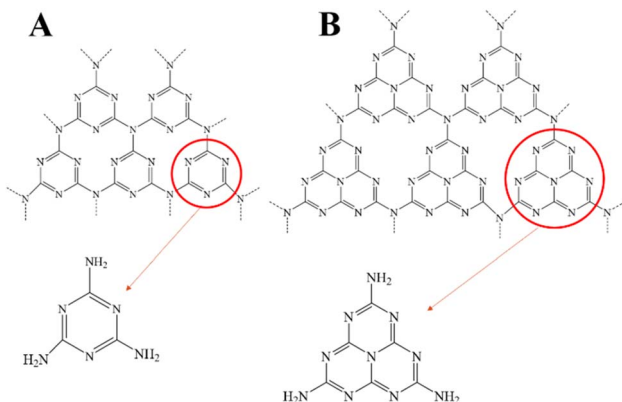


Fig. 2 Basic structure of  $\text{g-C}_3\text{N}_4$  (A) triazine ring (B) 3-s-triazine ring.

basic components of  $\text{g-C}_3\text{N}_4$  unit. As a non-metallic polymer semiconductor,  $\text{g-C}_3\text{N}_4$  has a band gap of 2.7 eV, strong visible light absorption, and is cheap and easy to obtain.<sup>19</sup> It is widely used in environmental and energy fields such as wastewater treatment,  $\text{CO}_2$  reduction, and hydrogen production by photolysis of water.<sup>20,21</sup> However, the main defects of  $\text{g-C}_3\text{N}_4$  are low specific surface area, low visible light absorption and high photogenerated electron hole recombination rate, which inhibit its photocatalytic activity to some extent.<sup>22,23</sup> The researchers focused on modifying  $\text{g-C}_3\text{N}_4$  in different ways to enhance its photocatalytic performance.

The properties of  $\text{g-C}_3\text{N}_4$ -based photocatalysts are affected by their microstructure. Structural engineering such as controlling shape and size is an important way to improve the photocatalytic ability of  $\text{g-C}_3\text{N}_4$ . Various methods can enlarge the specific surface area. In a simple two-step calcination procedure, Liang *et al.* created carbon vacancy-modified  $\text{g-C}_3\text{N}_4$  ( $\text{VC-C}_3\text{N}_4$ ) catalysts and used them for the first time to degrade bisphenol A (BPA) using photocatalysis.<sup>24</sup> Compared with pure  $\text{g-C}_3\text{N}_4$ ,  $\text{VC-C}_3\text{N}_4$  had significantly improved photocatalytic degradation activity for BPA, and its kinetic constant for BPA degradation was 1.65 times higher. The enhanced photocatalytic performance is mainly attributed to the carbon vacancies in  $\text{VC-C}_3\text{N}_4$ . Different  $\text{g-C}_3\text{N}_4$  preparation procedures frequently accompany defects, but it is still challenging to control the location of defects precisely. From the structural characteristics of the prepared  $\text{g-C}_3\text{N}_4$ , the post-treatment strategy has apparent advantages.<sup>25</sup>

Modifications in electron transport and the active site result from morphological changes. The unique morphology can boost the carrier's specific surface area and transfer rate.<sup>26</sup> The morphology and structure of  $\text{g-C}_3\text{N}_4$  can be changed by adjusting different reaction conditions, such as: sheet,<sup>27-29</sup> porous,<sup>30</sup> nanorods,<sup>31,32</sup> nanotube,<sup>33</sup> etc., thereby, the specific surface area, the number of active sites, and the mobility of photogenerated carriers are improved. Luo *et al.* successfully created a three-dimensional network structure photocatalyst (3D  $\text{g-C}_3\text{N}_4$  NR) made of  $\text{g-C}_3\text{N}_4$  nanorods.<sup>34</sup> The catalyst exhibited faster carrier transfer kinetics and higher specific surface area. Therefore, the phenol degradation efficiency of 3D

$\text{g-C}_3\text{N}_4$  NRs is significantly improved. Using melamine sponge (MS) and urea, Tang *et al.* successfully synthesized floating porous  $\text{g-C}_3\text{N}_4$  (FPCN) by a facile one-pot method, and the highest degradation efficiency of FPCN for tetracycline (TC) reached 70% without any stirring, which is 1.9 times the degradation efficiency of pure  $\text{g-C}_3\text{N}_4$ .<sup>35</sup> Its 3D interconnected network and improved light absorption are credited with its good photocatalytic activity. The increase of the specific surface area and the decrease of the photoinduced electron-hole pair recombination rate are the main reasons for improving the photocatalytic activity.

When  $\text{g-C}_3\text{N}_4$  is coupled with other semiconductor materials with different properties, the heterojunction interface generates an internal electric field to induce the band bending,<sup>36,37</sup> so the formed close contact interface can significantly improve the transfer and separation of free charges and make up for the shortcomings of low visible light absorption. Generally, based on the charge transfer mechanism, Z-scheme and type II heterojunctions can truly separate photogenerated electrons and holes from space.<sup>38-40</sup> As shown in Fig. 3(a) and (b), the type II, Z and S type heterostructures show different charge transfer paths.<sup>41-43</sup> Therefore, one of the methods to enhance the catalytic efficiency of  $\text{g-C}_3\text{N}_4$  is to composite it with other materials with matching energy band structures to construct heterostructures. Yang *et al.* synthesized 3D layered  $\text{g-C}_3\text{N}_4/\text{BiOBr}$  (pgB) heterojunction by precipitation and electrostatic self-assembly.<sup>44</sup> The enhanced photocatalytic performance is attributed to the efficient separation of electron-hole pairs due to the close contact between pgB. Compared with type II heterojunction, Z-type heterojunction can achieve space charge separation and maintain the strong oxidation/reduction ability of a single component,<sup>40,41</sup> and thus has received more attention and research. Cui *et al.* successfully prepared silver vanadate quantum dot ( $\text{AgVO}_3$  QD) doped reduced graphene oxide (RGO) and  $\text{g-C}_3\text{N}_4$  nanocomposite modified polyvinylidene fluoride (PVDF) thin film ( $\text{AgVO}_3/\text{RGO/CN-PVDF}$ ) to improve the photocatalytic activity.<sup>45</sup> Its unique 0D/2D/2D Z-scheme

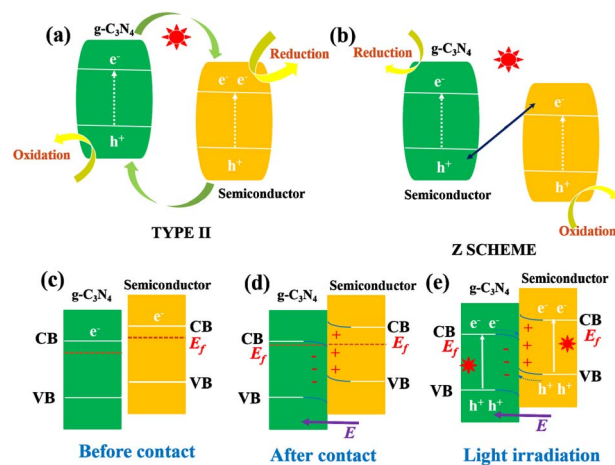


Fig. 3 Schematic representation of typical type II (a) and Z heterostructures (b), charge-transfer processes in an S-scheme heterojunction before contact (c), after contact (d), and light irradiation (e).

heterostructure and the pores of the PVDF framework synergistically improve the separation and transport of photo-generated carriers and promote the catalyst's ability to degrade pollutants. Yu *et al.* introduced a step-scheme (S-scheme) heterojunction consisting of a reduction photocatalyst (RP) and an oxidation photocatalyst (OP) with a staggered band structure.<sup>42</sup> It can be observed in Fig. 3(e) that the charge transfer path in the S-scheme mode is similar to a "step" in the macro sense and the letter N in the micro sense, which is the origin of its name. Xia *et al.* constructed a 0D/2D S scheme heterojunction material containing CeO<sub>2</sub> quantum dots and polymerized carbon nitride (CeO<sub>2</sub>/PCN).<sup>46</sup> The photocatalytic removal rate of the material against *Staphylococcus aureus* was 88.1%, 2.7 times and 8.2 times of that of pure CeO<sub>2</sub> (32.2%) and PCN (10.7%), respectively.

Various modification techniques enhanced the catalytic performance of g-C<sub>3</sub>N<sub>4</sub> in various ways. Among them, the main objective of morphology control is to increase the specific surface area and reduce the thickness; doping can change the band gap width; the construction of heterojunction is to promote carrier migration and expand the absorption range of visible light. At present, there are many ways to modify carbon nitride, but few ways to combine it with peroxidase, so we can further try to combine it with peroxidase to provide more choices.

### 3. Immobilization of HRP

Horseradish peroxidase (HRP) was originally discovered from the roots of the horseradish plant, hence the name horseradish peroxidase. HRP is a secreted plant peroxidase, which is in high demand in the market, with high stability and water solubility.<sup>47</sup> Currently, HRP can catalyze refractory organic pollutants only in the presence of H<sub>2</sub>O<sub>2</sub>,<sup>48,49</sup> and the degraded organic pollutants include anilines, hydroxyquinolines, carcinogenic aromatic amines, *etc.*<sup>9,48–52</sup> One challenge in applying HRP to the industry is avoiding the direct use of free enzymes.<sup>53–55</sup> Due to the disadvantages of free enzymes, such as poor operational stability, poor storage stability, environmental sensitivity, easy inactivation of enzyme molecules, and difficulty in recycling, it is difficult to reuse them in practical applications.<sup>50</sup> Therefore, finding an appropriate way to overcome this situation remains a hot issue. Immobilization of HRP is currently the most effective way to solve this problem. Enzyme immobilization technology is a biological technology that confines the natural free enzyme in a certain space or is wholly attached to a solid structure and cannot move freely.<sup>53</sup> It is a commonly used, effective and convenient biological enzyme modification method. The enzyme's catalytic activity and operational stability have both been considerably boosted. Fig. 4 visually shows the advantages of immobilized enzymes in catalytic reactions compared to free enzymes.

A type of technology known as enzyme immobilization binds or limits the enzyme in a specific area with a carrier material to preserve its catalytic activity, enhance its stability, and achieve reusability. Technology for enzyme immobilization has advanced significantly in recent years. As shown in Fig. 5, the

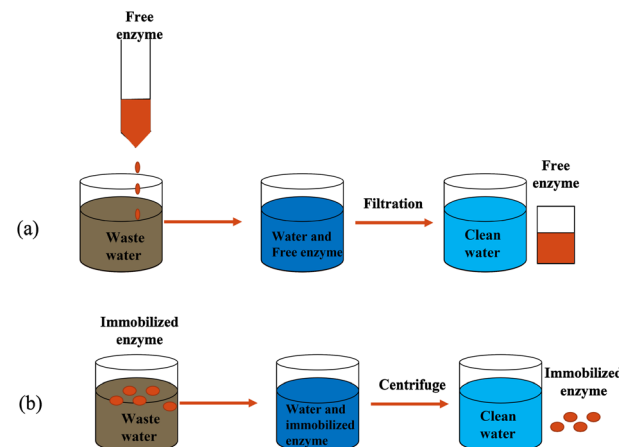


Fig. 4 The illustration of reactions catalysed between (a) free enzymes and (b) immobilized enzyme.

methods of immobilizing enzymes can be divided into two categories: physical methods and chemical methods.

Physical adsorption method uses various sorbents such as activated carbon, alumina and ion exchange resin to adsorb enzymes to the surface, so that the enzymes are connected with hydrogen bonds, ionic bonds and van der Waals forces on the substrate surface to immobilize free enzymes.<sup>56,57</sup> Pang *et al.* immobilized laccase on a synthetic bimodal micro-mesoporous Zr metal-organic framework (Zr-MOF, MMU) by physical adsorption.<sup>58</sup> Compared with free laccase, the immobilized system has larger adsorption capacity, wider pH and temperature distribution, better stability and reproducibility. Physical adsorption is the most traditional immobilization method, which has the advantages of mild conditions, simple operation, and less loss of enzyme activity.<sup>59,60</sup> However, because the adsorption process is reversible, the binding force to the carrier is weak, which will cause the enzyme to fall off easily during use.

Embedding immobilized enzyme has the characteristics of simple operation, low price, mild reaction conditions and slight loss of enzyme activity. Embedding methods usually require the embedding material and enzyme to be shaped during the immobilization process. Furthermore, during the embedding

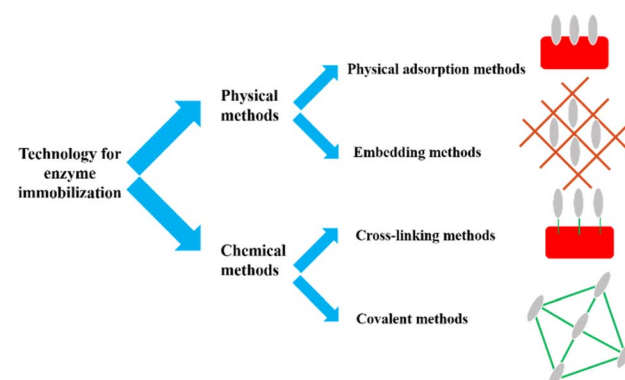


Fig. 5 Techniques for enzyme immobilization.



process, enzymes are often kept away from harsher environments. Under the protection of the embedded layer, the stability of the enzyme is improved. Aldhahri *et al.* reported the immobilization of HRP on copper oxide nanosheet (CuONS) *via* polymethyl methacrylate (PMMA) encapsulation.<sup>61</sup> The HRP activity recovered with 1% CuONS-PMMA was 72.8%. Over 50% of the enzyme activity was retained after repeated use for ten cycles. However, because the reaction substrate needs to enter the embedding layer to react with the enzyme, mass transfer resistance is an inherent problem of the embedding method, so the substrate affinity is often worse than that of the free enzyme.<sup>62</sup>

The cross-linking method uses a cross-linking agent to connect the enzyme molecule with the amino group, carboxyl group, epoxy group, *etc.* on the surface of the carrier by chemical reaction, to realize the immobilization of the enzyme. Meanwhile, the cross-linking method is usually combined with the adsorption method to fix the network structure obtained by cross-linking. Direct cross-linking of cross-linking agent and enzyme refers to the preparation of cross-linked aggregates or enzyme crystals with bifunctional reagents to prepare carrier-free large particles to obtain immobilized enzymes.<sup>13</sup> Bilal *et al.* used NHS as a cross-linking agent to immobilize HRP in a robust agarose-chitosan hydrogel (AHC-HRP).<sup>63</sup> ACH-HRP maintained better activity in acidic environments, good stability in alkaline conditions, and maintained 3.9 times more activity than its free counterpart at pH 10. At 70 °C, the catalytic capacity of the immobilized HRP was increased by a factor of 4. The use of carriers inevitably leads to activity dilution and introducing a large number of non-catalytic ballast leads to low space-time yield and productivity. Moreover, this problem cannot be alleviated by using a higher enzyme load, because when some enzyme molecules are too enriched on the surface of the carrier to form multilayer stacks or are located in deep positions in the carrier pores, the substrate will be difficult to approach the active center of the enzyme, resulting in the reduction of activity.

The covalent bonding method uses functional groups on the surface of the carrier, such as porous glass, agarose and porous silica, to chemically react with the amino and carboxyl groups in the enzyme molecule to form a covalent bond, thereby immobilizing the enzyme. Due to the strong valence bond formed, the reduction of enzyme activity during use is much less than that of other methods, and it is a commonly used immobilization method at present. Xue *et al.* co-immobilized HRP and syringaldehyde (SY) on glycidyl methacrylate and dopamine-grafted calcium alginate composite microspheres (PDGC).<sup>50</sup> The degradation rate of indole by HRP/PDGC-SY reaches 100%, which is 19.6 times that of free HRP. The degradation rate remained at 91.8% after repeated use for four cycles. However, the covalent binding of enzyme and carrier also has some defects. The enzyme and carrier will generally become unusable if the enzyme is irreversibly inactivated in the reaction. Stable covalent bonds sometimes make the enzyme in an unfavorable conformation, but reduce its activity.

In conclusion, compared with traditional methods, immobile HRP treatment technology is a reliable and promising tool

for effective treatment of wastewater. Compared with free HRP, immobilized HRP significantly improved the catalytic efficiency, excellent storage and operational stability, and allowed the recovery and reuse of enzymes. Recent studies have shown that adding photocatalyst to immobilized enzymes can have a great impact on enzyme wastewater treatment technology. Photocatalysts are promising enzyme immobilization supports for practical applications due to their unique structures and properties. Therefore, immobilizing peroxidase on photocatalysts is expected to be a future development prospect.

## 4. Photo-enzyme-coupled catalytic system

Photocatalysis and enzymatic treatment are two common organic pollutant wastewater treatment methods, but both are limited in some aspects. The reason for the high treatment cost is that it is more impractical to only use photocatalytic technology to treat wastewater with large volume and high pollutant concentration; in practical application of enzyme treatment method, it is necessary to consider the loss of enzyme and the impact of environmental changes on enzyme activity. In addition, it is necessary to consider adding intermediate mediators and H<sub>2</sub>O<sub>2</sub> when using HRP to treat wastewater, and the intermediate mediators have problems such as high cost and environmental toxicity. Therefore, in view of their respective advantages and disadvantages, the research on applying the two treatment methods to the treatment of wastewater after a reasonable combination has attracted the attention of scholars at home and abroad. By combining the characteristics of photocatalysis and enzyme treatment, the shortcomings of one of the two methods were made up, such as the low utilization of light energy in photocatalytic oxidation and the need of intermediate mediators in enzymes' reactions.

Photo-enzyme-coupled catalysis integrates high selectivity of enzyme catalysis and unique reactivity of photocatalysis to solar chemical conversion. The history of development of photo-enzyme-coupled catalysis is shown in Fig. 6. The combination of enzyme catalysis and natural photosynthesis represents the emergence of photo-enzyme-coupled catalysis. By the early 1960s, partially purified hydrogenase was used with spinach chloroplasts for solar driven H<sub>2</sub> evolution.<sup>64</sup> With the development of semiconductor photocatalysis, hydrogenase was combined with semiconductor in 1980s.<sup>65</sup> Compared with the photosynthesis of chloroplasts, photocatalysis can obtain solar energy more effectively, ensuring that the photo-enzyme-coupled catalysis can achieve efficient solar driven chemical conversion. In the early 2010's, more enzymes were discovered and the in-depth understanding of enzyme structure led to a more comprehensive development of the coupling system of photo enzyme catalysis.<sup>66</sup> The photo-enzyme-coupled catalysis has been successfully used in CO<sub>2</sub> reduction, N<sub>2</sub> fixation, H<sub>2</sub> production and the synthesis of value-added chemicals.<sup>67–70</sup> Compared with traditional enzyme catalysis, the hybrid system combines the remarkable catalytic function of enzyme with the advantages of photocatalysis, and has enhanced catalytic



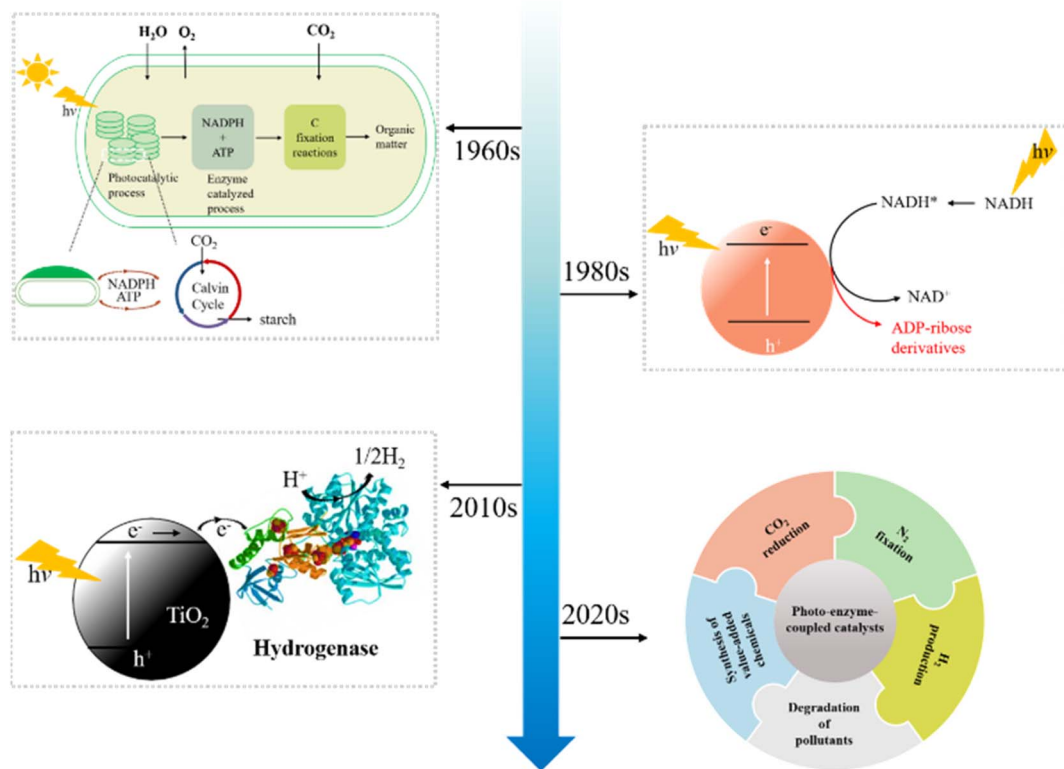


Fig. 6 Development of photo-enzyme-coupled catalysts.

efficiency, energy conversion efficiency and sustainable development.<sup>71</sup>

In recent years, researchers have proposed the concept of photo-enzyme-coupled catalysis, which mimics the principle of photosynthesis. The photo-enzyme-coupled catalysis system

consists of an independently regulated enzyme catalytic system and a photocatalyst. As shown in Fig. 7, the photocatalyst receives light and absorbs light energy, resulting in charge separation and the generation of electron hole pairs. The excited electrons are transferred to the enzyme active center to provide electrons and energy for the enzyme catalytic degradation of pollutants.<sup>72</sup> The photo-enzyme-coupled catalytic system represents a new development direction in the field of biocatalysis. It has the following remarkable characteristics: (1) mild degradation conditions of pollutants, low energy consumption, and less final products, which meet the requirements of green chemistry and sustainable development. (2) The construction process is simple and controllable, and can be used for different enzymatic reactions to achieve efficient degradation of different organic pollutants (3) coordination and optimization of photocatalysis and enzyme catalysis process, photocatalysis for enzyme catalysis to provide electrons and energy, can achieve complete degradation of organic pollutants.

Daâssi *et al.* investigated the catalytic conversion of BPA by different laccases, and the analysis by gas chromatography-mass spectrometry (GC-MS) showed that carboxylic acid derivatives such as tartaric acid were found to be BPA degradation products.<sup>73</sup> Zhang *et al.* prepared photo-enzyme heterojunction MCN/HRP-PEH to degrade BPA, and analysed the possible intermediates and final products by GC-MS. The intermediates were maleic acid and butanol, and the final products were small molecules such as CO<sub>2</sub> and H<sub>2</sub>O.<sup>14</sup> Dong *et al.* prepared Bi<sub>2</sub>WO<sub>6</sub>/HRP photo-enzyme catalyst to catalyse the degradation of

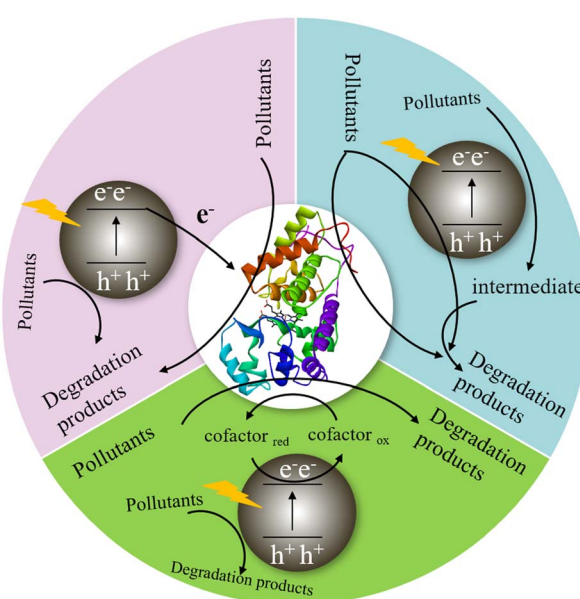


Fig. 7 Schematic diagram of different modes of photo-enzyme-coupled catalytic system.

BPA.<sup>74</sup> After 90 min detection by GC-MS, it was found that all the intermediates were completely degraded and mineralized, and finally degraded into  $\text{CO}_2$  and  $\text{H}_2\text{O}$ . The photo-enzyme-coupled catalysis will completely degrade and mineralize the pollutants to avoid the secondary environmental pollution caused by the new products catalysed by the enzyme.

The oxidoreductase is coupled with a semiconductor photocatalyst to construct a photo-enzyme-coupled catalytic system, which provided a new method for degrading organic pollutants.<sup>75,76</sup> It can not only improve the light absorption capacity of photocatalysts and the separation efficiency of photogenerated carriers, but also enhance the tolerance of biological enzymes to the environment, thus greatly improving the degradation rate and efficiency of photocatalysts.<sup>77</sup> As shown in Fig. 8, in the photo-enzyme-coupled catalytic system, the photocatalyst captures solar energy to generate holes and photo-generated electrons, and the oxidoreductase receives the photo-generated electrons to complete the highly selective conversion of substrate, and finally achieve efficient degradation of pollutants. Among them, the electron transfer process between photocatalyst and oxidoreductase is the key.<sup>15</sup> For an efficient photo-enzyme-coupled catalytic system, the photogenerated

electrons should have sufficient energy to activate the active centre of the oxidoreductase, and there should be an efficient and suitable electron transfer path between photocatalysts and oxidoreductases to achieve rapid and directional electron transfer.<sup>74,78</sup>

Li *et al.* reported for the first time the immobilization of *Candida* lipase on carbon nitride nanosheets ( $\text{C}_3\text{N}_4\text{-NS}$ ),<sup>76</sup> and the resulting immobilized lipase ( $\text{C}_3\text{N}_4\text{-NS@CRL}$ ) demonstrated strong enzyme loading, pH flexibility, thermal stability, and recyclability. This work shows that  $\text{C}_3\text{N}_4$  can be used as a novel platform for the fixation of chemical and biocatalysts and the construction of biohybrid catalysts for cascades. Ji *et al.* constructed a composite catalyst system by immobilizing HRP in the nanostructure of  $\text{TiO}_2$  hollow nanofibers.<sup>79</sup> This catalyst system effectively avoids UV-induced enzyme inactivation compared with free HRP or  $\text{TiO}_2/\text{UV}$ , significantly improves the removal efficiency of  $\text{TiO}_2\text{-HRP}$  for 2, 4-DCP, especially at high concentrations, which can degrade 90%. This work shows that HRP can be immobilized with photocatalysts for more efficient biocatalysis. Therefore,  $\text{g-C}_3\text{N}_4$  and HRP can be combined into a photo-enzyme-coupled catalytic system, which integrates the selectivity of HRP catalysis and the unique reactivity of  $\text{g-C}_3\text{N}_4$  to

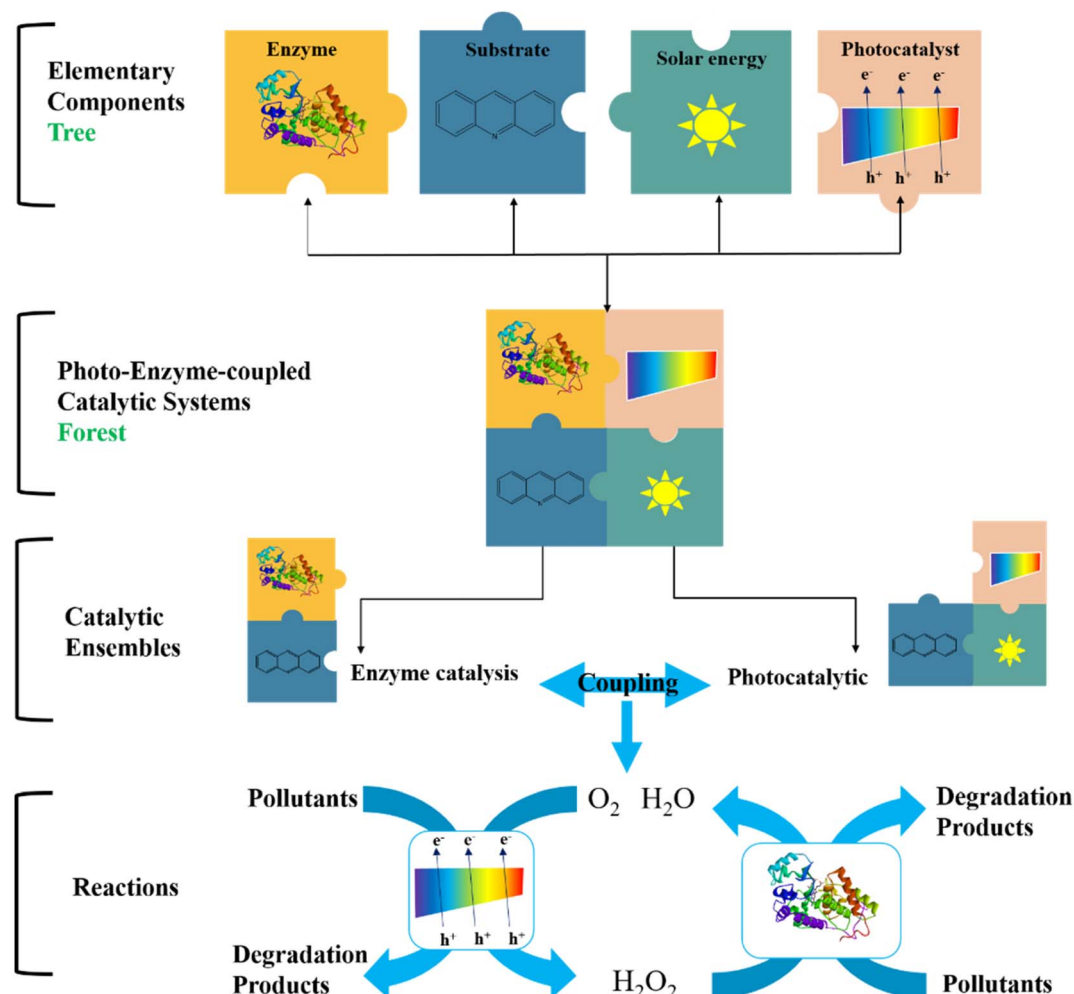


Fig. 8 Photo-enzyme-coupled catalysts systems.



Table 1 Effect of different photo-enzyme-coupled catalysts on pollutant degradation

Photocatalyst	Enzyme	Cross linking	Pollutants	Time	Degradation	Ref.
TiO <sub>2</sub>	CPO/HRP	Glutaraldehyde	Aniline blue, crystal violet	2 min	97.58%, 98.89%	82
TiO <sub>2</sub>	HRP	Emulsion electrospinning	2,4-DCP	180 min	90.00%	79
TiO <sub>2</sub>	Laccase	Bacterial cellulose	Reactive red X-3B dye	120 min	75.00%	75
g-C <sub>3</sub> N <sub>4</sub>	HRP	Nickel acetate solution	BPA, phenol, <i>p</i> -nitrophenol, 2-naphthol	60 min	97.90%, 99.99%, >80.00%, >85.00%	80
C <sub>3</sub> N <sub>4</sub> -NS	Candida rugosa lipase	Glutaraldehyde	<i>p</i> -Nitrophenol	—	—	76
MCN	HRP	Zn(OAc) <sub>2</sub>	BPA	50 min	85.70%	14
TiO <sub>2</sub>	Laccase	Adsorbent	2,4-DCP	210 min	59.10%	78
g-C <sub>3</sub> N <sub>4</sub>	HRP	Electrostatic assembly	MO	90 min	>90.00%	83
Bi <sub>2</sub> WO <sub>6</sub>	HRP	Electrostatic self-assembly process	BPA	90 min	84.50%	74
TiO <sub>2</sub>	Laccase	Cu	2,4-DCP	720 min	95.00%	15
g-C <sub>3</sub> N <sub>4</sub>	HRP	Cu <sub>3</sub> (PO <sub>4</sub> ) <sub>2</sub>	BPA	60 min	72.98%	81

degradation pollutants, and makes up for the shortcomings of low light energy utilization of g-C<sub>3</sub>N<sub>4</sub> and the need for intermediates in HRP reaction.

Li *et al.* have developed a novel nano biotic artificial catalytic system for g-C<sub>3</sub>N<sub>4</sub>/HRP. The degradation rate of BPA by g-C<sub>3</sub>N<sub>4</sub>/HRP reached 97.9% within 60 min, which was 13.2 times and 3.8 times that of single HRP (7.4%) and g-C<sub>3</sub>N<sub>4</sub> (25.9%), respectively.<sup>80</sup> Photo catalysis and enzymatic degradation of pollutants are carried out simultaneously to achieve the effect of mutual promotion. Since light can negatively affect enzyme activity, biological enzymes in this situation are easily inactivated by environmental influences, so it is necessary to protect the enzyme, such as using embedding method to fix the enzyme and prevent the enzyme from being directly oxidized. Zhang *et al.* prepared a photo-enzyme heterojunction MCN/HRP-PEH by immobilizing HRP on mesoporous g-C<sub>3</sub>N<sub>4</sub> (MCN).<sup>14</sup> The catalyst improves the carrier separation efficiency and visible light absorption ability of g-C<sub>3</sub>N<sub>4</sub>, and the highest degradation rate of BPA reaches 85.7%, which is 35.7 times and 1.8 times that of free HRP and MCN, respectively.

In order to exhibits excellent enzymatic ability of immobilized enzymes and be more tolerant to extreme acid, alkali and high temperature, Wu *et al.* firstly synthesized HRP and g-C<sub>3</sub>N<sub>4</sub> inorganic into nanoleaves to construct a photo-enzyme cascade catalytic system, namely HRP-CN/Cu<sub>3</sub>(PO<sub>4</sub>)<sub>2</sub> nanoleaves.<sup>81</sup> The encapsulation efficiency of HRP in the catalyst was up to 36.2%, and the degradation efficiency of BPA reached 73.0%. The participation of g-C<sub>3</sub>N<sub>4</sub> not only increased the loading of HRP, but also enhanced the enzymatic activity of immobilized HRP compared with conventional enzyme-inorganic hybrid nanoflower.

By comparing Table 1, it can be clearly seen that the degradation efficiency of 2,4-DCP by TiO<sub>2</sub>/HRP catalyst (90.00%) is much higher than that of TiO<sub>2</sub>/laccase (59.10%). The degradation efficiency of BPA by MCN/HRP catalyst (85.7%) after 50 min was much higher than that by Bi<sub>2</sub>WO<sub>6</sub>/HRP catalyst (84.6%) after 90 min. Compared with other inorganic semiconductor

materials, g-C<sub>3</sub>N<sub>4</sub> has a unique two-dimensional structure similar to graphene. It does not contain expensive precious metals and rare elements. The chemical structure can be controlled simply through doping, and the band structure can be accurately adjusted, greatly improving the utilization rate of light energy and quantum efficiency. The photo-enzyme-coupled catalytic degradation of pollutants also showed better results. The coupling of g-C<sub>3</sub>N<sub>4</sub> and HRP realized the synergistic effect of the two catalysts, which greatly improved the efficiency of carrier separation to continuously produce more ·OH active species, thereby realizing efficient non-selective degradation of various pops.

## 5. Conclusions

In this review, we mainly reviewed the modification methods of g-C<sub>3</sub>N<sub>4</sub> and the immobilization technology of HRP, constructed a g-C<sub>3</sub>N<sub>4</sub>-HRP-coupled catalytic system, and summarized its latest research progress. The catalytic process of HRP must have H<sub>2</sub>O<sub>2</sub>, but in the photo-enzyme cascade consisting of HRP and g-C<sub>3</sub>N<sub>4</sub> does not require additional H<sub>2</sub>O<sub>2</sub> and does not produce harmful intermediates, which can make full use of solar energy. In the synergistic system of HRP and g-C<sub>3</sub>N<sub>4</sub>, the participation of g-C<sub>3</sub>N<sub>4</sub> increased the loading of HRP and enhanced the enzymatic activity of immobilized HRP, the participation of HRP increased the reaction rate and accelerated the electron transport of g-C<sub>3</sub>N<sub>4</sub>. This system provides a new possibility for the photo-enzyme-coupled catalytic system, which is expected to be widely used in the fields of biosynthesis, medical treatment and environmental protection. Overall, the photo-enzyme-coupled catalytic system based on g-C<sub>3</sub>N<sub>4</sub> can be used successfully for efficient photo-enzyme catalysis and pollutant degradation using solar energy for sustainable development. Although the photocatalytic performance of g-C<sub>3</sub>N<sub>4</sub> and the enzymatic performance of HRP after photo-enzyme-coupled are greatly increased, the efficiency remains lower than envisaged, limiting their large-scale use and commercialization.



Therefore, the following efforts should be made to meet this challenge:

(i) When  $\text{g-C}_3\text{N}_4$  reacts with HRP, although the surrounding active site can promote conduction and accelerate the reaction process, it will inactivate the enzyme. So far, the mechanism of inactivation of photogenic holes and reactive oxygen species to enzymes has been preliminarily established, and several protective methods have been demonstrated. Therefore, it is necessary to further elucidate the inactivation mechanism of the enzyme to obtain more effective protection strategies and improve the stability of the enzyme.

(ii) Inspired by the structure and function of enzymes, the design of efficient and stable catalysts may be an important direction. Reduced graphene oxide (RGO) was found to efficiently consume  $\cdot\text{O}_2^-$ , thereby improving HRP stability in  $\text{H}_2\text{O}_2$  reactions. Therefore, the photo-enzyme-coupled catalytic system based on  $\text{g-C}_3\text{N}_4$  can select materials with high surface area and biocompatibility to construct new electron transfer channels.

(iii) Although the visible photo absorption ranges of the photo-enzyme-coupled catalytic system based on  $\text{g-C}_3\text{N}_4$  extends to longer wavelengths, in order to better utilize the complete solar spectrum, it is expected to further increase the absorption range by adjusting the ratio of photo catalyst to enzyme catalyst, even to the near infrared.

(iv) Although the  $\text{g-C}_3\text{N}_4$ -based photo-enzyme-coupled catalytic system can achieve good charge separation and migration when in close contact, the main challenge now is to understand the charge separation and the mechanism of the process to further promote the development of photo enzyme coupled catalytic system. The performance of  $\text{g-C}_3\text{N}_4$  is largely influenced by the material and structure design used. A reasonable structure helps to improve the immobilization and stability of HRP, while making more efficient use of solar energy, facilitating its own electron separation and transport, and accelerating surface reactions. Therefore, the structure and performance of  $\text{g-C}_3\text{N}_4$  can be adjusted by varying degrees of modification.

(v) Numerous recent studies have demonstrated that  $\text{g-C}_3\text{N}_4$ -based photo-enzyme-coupled catalytic systems are versatile candidates in photo catalysis, enzymatic catalysis, and electrochemistry. Although the current system has been extensively studied in the degradation of pollutants in the environment, it is necessary to further investigate other aspects, such as  $\text{CO}_2$  reduction and organic matter synthesis, in the future.

## Conflicts of interest

The authors declare that they have no known competing financial interests or personal relationships that could have appeared to influence the work reported in this paper.

## Acknowledgements

This work was financially supported by the Key Research and Development Projects of Ningxia Province of China (2021BEB04055, 2020BEG03033, 2022BDE03013), Natural

Science Foundation of Ningxia (2022AAC03146, 2021AAC03056), CAS "Light of West China Program" of China (XAB2020YW16), and School-level Special Talents Launching Project of Ningxia Medical University (XT2020017).

## Notes and references

- Q. Wang and Z. Yang, *Environ. Pollut.*, 2016, **218**, 358–365.
- R. P. Schwarzenbach, T. Egli, T. B. Hofstetter, U. von Gunten and B. Wehrli, *Annu. Rev. Environ. Resour.*, 2010, **35**, 109–136.
- K. Murtada, D. Bowman, M. Edwards and J. Pawliszyn, *Talanta*, 2022, **242**, 123301.
- Y. Lu, S. Song, R. Wang, Z. Liu, J. Meng, A. J. Sweetman, A. Jenkins, R. C. Ferrier, H. Li, W. Luo and T. Wang, *Environ. Int.*, 2015, **77**, 5–15.
- K. Wetchakun, N. Wetchakun and S. Sakulsermsuk, *J. Ind. Eng. Chem.*, 2019, **71**, 19–49.
- J. Xu, Y. Chen, Z. Dong, Y. Peng, Y. Situ and H. Huang, *Appl. Catal., B*, 2019, **252**, 41–46.
- T. H. Pham, J.-W. Park and T. Kim, *Sol. Energy*, 2021, **215**, 151–156.
- H. Xing, W. Wen and J.-M. Wu, *J. Photochem. Photobiol., A*, 2019, **382**, 111958.
- Y. Huang, J. Lin, J. Zou, J. Xu, M. Wang, H. Cai, B. Yuan and J. Ma, *Sci. Total Environ.*, 2021, **798**, 149276.
- A. Saravanan, P. S. Kumar, D.-V. N. Vo, S. Jeevanantham, S. Karishma and P. R. Yaashikaa, *J. Hazard. Mater.*, 2021, **419**, 126451.
- G. Bayramoglu and M. Y. Arica, *J. Hazard. Mater.*, 2008, **156**, 148–155.
- M. Bilal, T. Rasheed, H. M. N. Iqbal, H. Hu, W. Wang and X. Zhang, *Int. J. Biol. Macromol.*, 2017, **105**, 328–335.
- M. Petronijevic, S. Panic, S. Savic, J. Agbaba, J. Molnar Jazic, M. Milanovic and N. Durisic-Mladenovic, *Colloids Surf., B*, 2021, **208**, 112038.
- H. Zhang, J. Wu, J. Han, L. Wang, W. Zhang, H. Dong, C. Li and Y. Wang, *Chem. Eng. J.*, 2020, **385**, 123764.
- X. Cao, J. Gao, Y. Yang, H. Li, X. Zheng, G. Liu and Y. Jiang, *J. Environ. Chem. Eng.*, 2022, **10**, 107909.
- A. Fujishima and K. Honda, *Nature*, 1972, **238**, 37–38.
- J. H. Carey, J. Lawrence and H. M. Tosine, *Bull. Environ. Contam. Toxicol.*, 1976, **16**(6), 697–701.
- X. Wang, K. Maeda, A. Thomas, K. Takanabe, G. Xin, J. M. Carlsson, K. Domen and M. Antonietti, *Nat. Mater.*, 2009, **8**, 76–80.
- Y. Zheng, L. Lin, B. Wang and X. Wang, *Angew. Chem., Int. Ed.*, 2015, **54**, 12868–12884.
- J. Fu, Q. Xu, J. Low, C. Jiang and J. Yu, *Appl. Catal., B*, 2019, **243**, 556–565.
- F. Guo, B. Hu, C. Yang, J. Zhang, Y. Hou and X. Wang, *Adv. Mater.*, 2021, **33**, e2101466.
- L. Cheng, H. Zhang, X. Li, J. Fan and Q. Xiang, *Small*, 2021, **17**, e2005231.
- J. Fu, J. Yu, C. Jiang and B. Cheng, *Adv. Energy Mater.*, 2018, **8**, 1701503.
- X. Liang, G. Wang, X. Dong, G. Wang, H. Ma and X. Zhang, *ACS Appl. Nano Mater.*, 2018, **2**, 517–524.



25 L. Jiang, J. Yang, X. Yuan, J. Guo, J. Liang, W. Tang, Y. Chen, X. Li, H. Wang and W. Chu, *Adv. Colloid Interface Sci.*, 2021, **296**, 102523.

26 J. Kröger, A. Jiménez-Solano, G. Savasci, V. W. h. Lau, V. Duppel, I. Moudrakovski, K. Küster, T. Scholz, A. Gouder, M. L. Schreiber, F. Podjaski, C. Ochsenfeld and B. V. Lotsch, *Adv. Funct. Mater.*, 2021, **31**, 2102468.

27 W. Ma, N. Wang, Y. Guo, L. Yang, M. Lv, X. Tang and S. Li, *Chem. Eng. J.*, 2020, **388**, 124288.

28 G. Lin, M. Duan, J. M. Perez-Aguilar, Z. Gu and Y. Tu, *Colloids Surf. B*, 2021, **205**, 111896.

29 X. Wu, X. Wang, F. Wang and H. Yu, *Appl. Catal., B*, 2019, **247**, 70–77.

30 Z. Liang, X. Zhuang, Z. Tang, Q. Deng, H. Li and W. Kang, *Chem. Eng. J.*, 2022, **432**, 134388.

31 V. Jayaraman, C. Ayappan and A. Mani, *Chemosphere*, 2022, **287**, 132055.

32 X.-H. Li, X. Wang and M. Antonietti, *Chem. Sci.*, 2012, **3**, 2170.

33 Q. Gao, Q. Lei, R. Miao, M. Gao, H. Liu, Q. Yang, Y. Liu, F. Song, Y. Yu and W. Yang, *New J. Chem.*, 2022, **46**, 3588–3594.

34 W. Luo, X. Chen, Z. Wei, D. Liu, W. Yao and Y. Zhu, *Appl. Catal., B*, 2019, **255**, 117761.

35 J. Tang, J. Wang, L. Tang, C. Feng, X. Zhu, Y. Yi, H. Feng, J. Yu and X. Ren, *Chem. Eng. J.*, 2022, **430**, 132669.

36 M. Humayun, H. Ullah, A. AliTahir, A. R. M. Yusoff, M. A. M. Teridi, M. K. Nazeeruddin and W. Luo, *Chem. Rec.*, 2021, **21**, 1811–1844.

37 H. Boumeriame, B. F. Machado, N. M. M. Moura, P. Serp, L. Andrade, T. Lopes, A. Mendes, T. Chafik, E. S. Da Silva and J. L. Faria, *Int. J. Hydrogen Energy*, 2022, **47**, 25555–25570.

38 U. Ghosh, A. Majumdar and A. Pal, *J. Environ. Chem. Eng.*, 2021, **9**, 104631.

39 W.-J. Ong, *Front. Mater.*, 2017, **4**, 1–10.

40 H. Yang, *Mater. Res. Bull.*, 2021, **142**, 111406.

41 Q. Xu, L. Zhang, J. Yu, S. Wageh, A. A. Al-Ghamdi and M. Jaroniec, *Mater. Today*, 2018, **21**, 1042–1063.

42 Q. Xu, L. Zhang, B. Cheng, J. Fan and J. Yu, *Chem.*, 2020, **6**, 1543–1559.

43 A. Shawky and R. M. Mohamed, *J. Environ. Chem. Eng.*, 2022, **10**, 108249.

44 L. Yang, L. Liang, L. Wang, J. Zhu, S. Gao and X. Xia, *Appl. Surf. Sci.*, 2019, **473**, 527–539.

45 Y. Cui, Z. Wang, J. Zheng, B. Li, Y. Yan and M. Meng, *J. Colloid Interface Sci.*, 2022, **614**, 677–689.

46 P. Xia, S. Cao, B. Zhu, M. Liu, M. Shi, J. Yu and Y. Zhang, *Angew. Chem., Int. Ed. Engl.*, 2020, **59**, 5218–5225.

47 H. Akbar, D. M. Sedzro, M. Khan, S. F. Bellah and S. M. S. Billah, *J. Chem. Environ. Biolo. Eng.*, 2018, **2**, 52–59.

48 Z. Shu, J. Wang, H. Liu and C. Liu, *Chem. Eng. J.*, 2022, **428**, 131132.

49 G. Bayramoglu, A. Akbulut and M. Y. Arica, *Chem. Eng. Res. Des.*, 2021, **165**, 435–444.

50 X. Liu, P. Xue, F. Jia, K. Shi, Y. Gu, L. Ma and R. Li, *Chemosphere*, 2021, **262**, 128411.

51 B. E. Keshta, A. H. Gmeay and A. A. Khamis, *Environ. Sci. Pollut. Res.*, 2022, **29**, 6633–6645.

52 O. T. Gül and I. Ocsoy, *Mater. Lett.*, 2021, **303**, 130501.

53 F. Shakerian, J. Zhao and S. P. Li, *Chemosphere*, 2020, **239**, 124716.

54 F. Jia, B. Narasimhan and S. Mallapragada, *Biotechnol. Bioeng.*, 2014, **111**, 209–222.

55 Z. Ashkan, R. Hemmati, A. Homaei, A. Dinari, M. Jamliidoost and A. Tashakor, *Int. J. Biol. Macromol.*, 2021, **168**, 708–721.

56 T. Jesionowski, J. Zdarta and B. Krajewska, *Adsorption*, 2014, **20**, 801–821.

57 D. Huang, B. Li, J. Ou, W. Xue, J. Li, Z. Li, T. Li, S. Chen, R. Deng and X. Guo, *J. Environ. Manage.*, 2020, **261**, 109879.

58 S. Pang, Y. Wu, X. Zhang, B. Li, J. Ouyang and M. Ding, *Process Biochem.*, 2016, **51**, 229–239.

59 D.-M. Liu, J. Chen and Y.-P. Shi, *Trends Anal. Chem.*, 2018, **102**, 332–342.

60 A. A. Homaei, R. Sariri, F. Vianello and R. Stevanato, *J. Chem. Biol.*, 2013, **6**, 185–205.

61 M. Aldhahri, Y. Q. Almulaiky, R. M. El-Shishtawy, W. M. Al-Shawafi, N. Salah, A. Alshahrie and H. A. H. Alzahrani, *Catal. Lett.*, 2020, **151**, 232–246.

62 D. A. M. Urrea, A. V. F. Gimenez, Y. E. Rodriguez and E. M. Contreras, *Process Saf. Environ. Prot.*, 2021, **156**, 134–143.

63 M. Bilal, T. Rasheed, Y. Zhao and H. M. N. Iqbal, *Int. J. Biol. Macromol.*, 2019, **124**, 742–749.

64 D. I. Arnon and A. M. A. Panque, *Science*, 1961, **134**, 1425.

65 V. V. Nikandrov, M. A. Shlyk, N. A. Zorin, I. N. Gogotov and A. A. Krasnovsky, *FEBS Lett.*, 1988, **234**, 111–114.

66 E. Reisner, D. J. Powell, C. Cavazza, J. C. Fontecilla-Camps and F. A. Armstrong, *J. Am. Chem. Soc.*, 2009, **131**, 18457–18466.

67 R. K. Yadav, J. O. Baeg, G. H. Oh, N. J. Park, K. J. Kong, J. Kim, D. W. Hwang and S. K. Biswas, *J. Am. Chem. Soc.*, 2012, **134**, 11455–11461.

68 W. Zhang, B. O. Burek, E. Fernandez-Fueyo, M. Alcalde, J. Z. Bloh and F. Hollmann, *Angew. Chem., Int. Ed.*, 2017, **56**, 15451–15455.

69 Y. Y. Zhang, Y. Zhao, R. Li and J. Liu, *Sol. RRL*, 2020, **5**, 2000339.

70 Y. Tan, J. Ma, F. Zhang, S. Wang, F. Lan, H. Liu and R. Li, *ACS Sustainable Chem. Eng.*, 2022, **10**, 12065–12071.

71 S. Zhang, S. Liu, Y. Sun, S. Li, J. Shi and Z. Jiang, *Chem. Soc. Rev.*, 2021, **50**, 13449–13466.

72 N. Yang, Y. Tian, M. Zhang, X. Peng, F. Li, J. Li, Y. Li, B. Fan, F. Wang and H. Song, *Biotechnol. Adv.*, 2022, **54**, 107808.

73 D. Daâssi, A. Prieto, H. Zouari-Mechichi, M. J. Martínez, M. Nasri and T. Mechichi, *Int. Biodeterior. Biodegrad.*, 2016, **110**, 181–188.

74 H. Dong, N. Song, M. Yan, H. Wu, H. Zhang, C. Ma and Y. Wang, *Chin. Chem. Lett.*, 2021, **32**, 2047–2051.

75 G. Li, A. G. Nandaonkar, Q. Wang, J. Zhang, W. E. Krause, Q. Wei and L. A. Lucia, *J. Membr. Sci.*, 2017, **525**, 89–98.

76 Y. Li, Z. Ruan, M. Zheng, Q. Deng, S. Zhang, C. Zheng, H. Tang, F. Huang and J. Shi, *RSC Adv.*, 2018, **8**, 14229–14236.



77 Z. Gong, Y. Yang, M. Wang, K. Lu, P. Liu, H. Wang and S. Gao, *Sci. Total Environ.*, 2020, **704**, 135246.

78 Y. Zhang, J. Gao, X. Xin, L. Wang, H. Li, X. Zheng and Y. Jiang, *Appl. Mater. Today*, 2020, **21**, 100810.

79 X. Ji, Z. Su, M. Xu, G. Ma and S. Zhang, *ACS Sustainable Chem. Eng.*, 2016, **4**, 3634–3640.

80 C. Li, S. Yu, L. Gu, J. Han, H. Dong, Y. Wang and G. Chen, *Adv. Mater. Interfaces*, 2018, **5**, 1801297.

81 J. Wu, X. Ma, C. Li, X. Zhou, J. Han, L. Wang, H. Dong and Y. Wang, *Chem. Eng. J.*, 2022, **427**, 131808.

82 H. Cheng, M. Hu, Q. Zhai, S. Li and Y. Jiang, *Chem. Eng. J.*, 2018, **347**, 703–710.

83 J. Bian, X. An, W. Jiang, R. Liu, C. Hu and H. Liu, *Chem. Eng. J.*, 2021, **408**, 127231.

